

## HYDRODYNAMICAL SURVEY OF FIRST OVERTONE CEPHEIDS

MICHAEL FEUCHTINGER<sup>1</sup>, J. ROBERT BUCHLER<sup>1</sup> & ZOLTÁN KOLLÁTH<sup>2</sup>

*ASTROPHYSICAL JOURNAL, submitted*

### ABSTRACT

A hydrodynamical survey of the pulsational properties of first overtone Galactic Cepheids is presented. The goal of this study is to reproduce their observed light- and radial velocity curves. The comparison between the models and the observations is made in a quantitative manner on the level of the Fourier coefficients. Purely radiative models fail to reproduce the observed features, but convective models give good agreement.

It is found that the sharp features in the Fourier coefficients are indeed caused by the  $P_1/P_4 = 2$  resonance, despite the very large damping of the 4th overtone. For the adopted mass-luminosity relation the resonance center lies near a period of  $4^d2 \pm 0.3$  as indicated by the observed radial velocity data, rather than near  $3^d2$  as the light-curves suggest.

*Subject headings:* turbulence, convection, hydrodynamics, oscillations of stars - Cepheids - s Cepheids  
 - convection

<sup>1</sup>Physics Department, University of Florida, Gainesville, FL, USA; buchler@physics.ufl.edu

<sup>2</sup>Konkoly Observatory, Budapest, HUNGARY; kollath@konkoly.hu

### 1. INTRODUCTION

Historically, s Cepheids denote a certain type of low amplitude Cepheids with almost sinusoidal light-curves. Recently, the large microlensing surveys EROS (Beaulieu *et al.* 1995), MACHO (Welch *et al.* 1995) and OGLE (Udalski *et al.* 1997) have confirmed unequivocally that these stars are overtone Cepheids. The vast majority are first overtone pulsators that coexist with a few second overtone Cepheids at the lower period end.

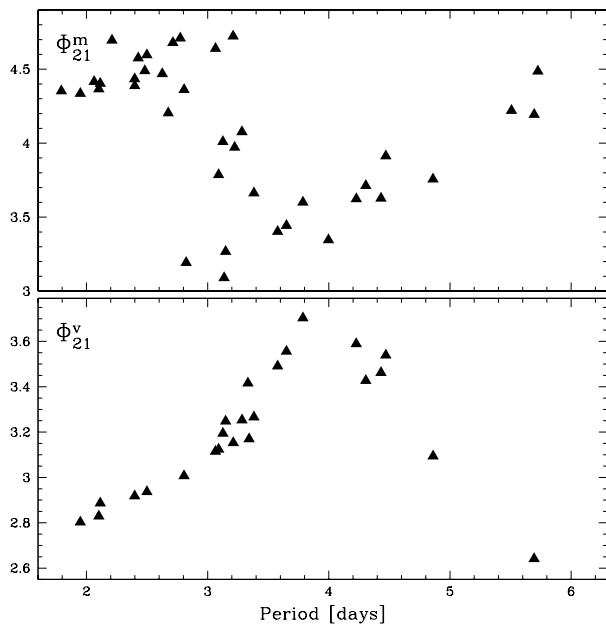


Fig. 1: Observational phase difference  $\Phi_{21}$  of Galactic first overtone Cepheids: light-curves [mag] (upper panel) and radial velocity curves (lower panel).

For a comparison between the observational data and the calculated model pulsations a Fourier decomposition provides an accurate quantitative representation. A salient feature in the Galactic first overtone Cepheid light-curve data (labelled with a superscript m) is a large and sharp drop of the Fourier phase difference  $\Phi_{21}^m$  as a function of period in the vicinity of the  $3^d2$  period. The upper panel of Fig. 1 shows the observational data summarized in Poretti (1994), and supplemented with V351 Cep and Anon C Mon (Moskalik, priv. comm.). The additional Fourier data are displayed as solid triangles in the left panel of Fig. 3. The quantity  $\Phi_{31}^m$  exhibits a more or less monotonic, but large  $\approx 2\pi$  rise. The amplitude ratios  $R_{21}^m$  and  $R_{31}^m$  display a local minimum in the same vicinity.

A large set of Galactic Cepheid radial velocity data has recently become available (Kienzle *et al.* 1999, Krzyt *et al.* 2000). The phase difference  $\Phi_{21}^v$  for the radial velocity (superscript v) is plotted in the lower panel of Fig. 1, and the other Fourier coefficients are displayed as solid triangles in the left column of Fig. 3.

Rapid variations in the Fourier phases are not special to the first overtone Cepheids. Actually, one of the striking features of the classical (fundamental mode) Cepheids is a Hertzsprung progression of these phases, so named after the concomitant bump progression that Hertzsprung (1926) noticed in the shape of the light-curves. For the classical Cepheids the center of this progression lies in the vicinity of the 10 day period. It was conjectured by Simon & Schmidt (1976) that this progression might have its origin in the presence of a  $P_0/P_2 = 2$  resonance between the fundamental mode of oscillation and the second overtone. This conjecture was later put on a solid mathematical basis with the help of the amplitude equation formalism (Buchler & Goupil 1984, Buchler & Kovács 1986, Kovács & Buchler 1989) and was confirmed with concomitant nu-

merical hydrodynamical modelling (Buchler, Moskalik & Kovács 1990, Moskalik, Buchler & Marom 1992).

In fact, it is now well established mathematically that sharp features in the Fourier coefficients, such as those observed in Cepheids and BL Herculis stars, are due to the appearance of resonances of the excited mode with an overtone at certain pulsation periods (*e.g.*, Buchler 1993, Buchler 2000). Conversely the lack of such structure as in RR Lyrae is indicative of the absence of resonances.

Subsequently, Antonello & Poretti (1986), from the behavior of  $\Phi_{21}^m$  and  $R_{21}^m$  with period (Fig. 3) and from the analogy with the Fourier data of the fundamental Cepheids, have suggested that a similar resonance, *viz.*  $P_1/P_4 = 2$  is operative in the first overtone Cepheids and is located near  $P_1 = 3^{\text{d}}.2$ . However, Kienzle *et al.* (1999), on the basis of the corresponding radial velocity data, suggest that the resonance center lies at a much higher period, closer to  $4^{\text{d}}.6$ . This incongruity suggests that it is dangerous to guess the location of a resonance without proper theoretical input. We will discuss this point further below.

In contrast to the fundamental Cepheids, the first overtone Cepheid pulsators have only received scant theoretical attention. Aikawa *et al.* (1987) computed the radial velocity and light curves of 11 radiative overtone pulsator models with the specific purpose of reproducing the observations of SU Cas, but were not satisfied with their results. (One labels radiative models in which convective heat transport is disregarded). Later, Antonello & Aikawa (1993) calculated two short sequences of Cepheids in order to see if numerical hydrodynamic modelling would confirm the postulated role of the  $P_1/P_4 = 2$  resonance in the vicinity of 3 days. Their results displayed some structure near the resonance, but failed to reproduce the observed structure in the Fourier coefficients, in particular the  $\Phi_{21}^m$  variation. The number of computed models was rather limited, and artificially enhanced opacities were used. Subsequently, Schaller & Buchler (1994), on the basis of an extensive study of radiative first overtone Cepheids with the OPAL opacities, reached the conclusion that radiative models cannot reproduce the observed structure of the Fourier coefficient  $\Phi_{21}^m$ ; a similar conclusion was also reached by Antonello & Aikawa (1995). This disagreement with observation came as a surprise considering how well the fundamental mode Galactic Cepheid pulsations can be modelled (*e.g.*, Moskalik, Buchler & Marom 1992).

In the last few years a lot of effort has been devoted to including convection in the pulsation codes, and recently one of the major remaining challenges, namely the modelling of beat pulsations, has been met (*e.g.*, Kolláth *et al.* 1998, Feuchtinger 1998). In this paper we apply the same convective codes to the study of first overtone pulsations.

## 2. PHYSICAL INPUT

Linear and nonlinear models are calculated with the Vienna pulsation code (Feuchtinger 1999a), which solves the equations of radiation hydrodynamics together with a time-dependent model equation for turbulent convection. This code recently has been extended by a linear nonadiabatic normal mode analysis, details of which are presented in a separate paper. For comparison purposes some of the calculations that are described in this paper have also been performed in parallel with the Florida pulsation code (de-

scribed in Kolláth, Buchler, Szabó & Csabry 2000). The latter uses a different numerical approach, but with only minor differences in the input physics. We have ascertained that the two codes give basically the same results.

For the Rosseland mean of the opacity we use the most recent OPAL tables (Iglesias & Rogers 1996) which are augmented by the Alexander & Ferguson (1994) low temperature opacities below 6000 K. The Eddington factor is set to  $1/3$ .

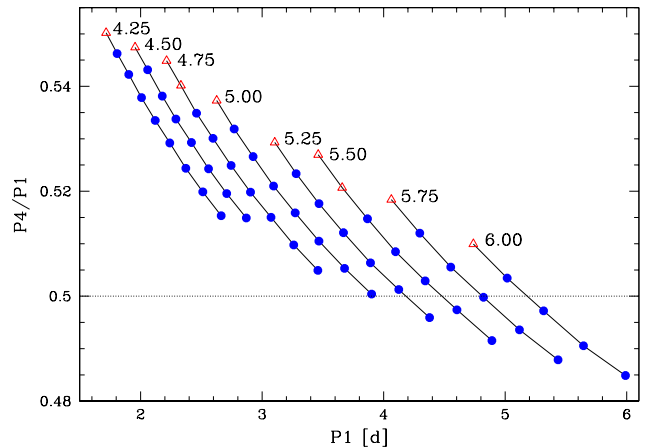


Fig. 2: Period ratio  $P_4/P_1$  versus pulsation period for radiative models. Open triangles refer to vibrationally stable models and filled circles to models which have a stable limit-cycle. Labels on top indicate the stellar mass of the corresponding sequence.

Our *model sequences* have constant mass and luminosity and an equilibrium effective temperature varying in steps of 100 K. They represent horizontal paths through the instability strip (IS). We adopt a mass–luminosity (ML) relation:  $\log(L/L_\odot) = 0.79 + 3.56 \log(M/M_\odot)$ , which is derived from the stellar evolution calculations of Schaller *et al.* (1992) which make use of the same OPAL opacity data. For a good coverage of the observed period range we vary the stellar mass between 4.25 and 6.5  $M_\odot$  in steps of 0.25  $M_\odot$ . The chemical composition corresponds to a typical Galactic one of  $(X, Y, Z) = (0.70, 0.28, 0.02)$ .

The Fourier decomposition of the resulting light- and radial velocity curves is calculated by a least squares fit with a standard Fourier sum (8 terms). Amplitude ratios  $R_{n1} = A_n/A_1$  and phase differences  $\Phi_{n1} = \Phi_n - n\Phi_1$  are then used for the comparison to the observed data. Following custom, a cos Fourier decomposition is used for the light-curve data, and a sin decomposition for the radial velocity data. Note further that we compute bolometric light variations, which are compared to V-band magnitudes. For the case of RR Lyrae stars it has been shown that the differences in the low order Fourier coefficients between bolometric and V light-curves are rather small, in particular for low amplitude first overtone pulsations (Dorfi & Feuchtinger 1999, Feuchtinger & Dorfi 2000). However, for metal-rich Galactic Cepheids this has to be checked by detailed radiative transfer calculations, which will be done in a companion paper.

For the transformation between theoretical and observed radial velocities we apply a constant projection and

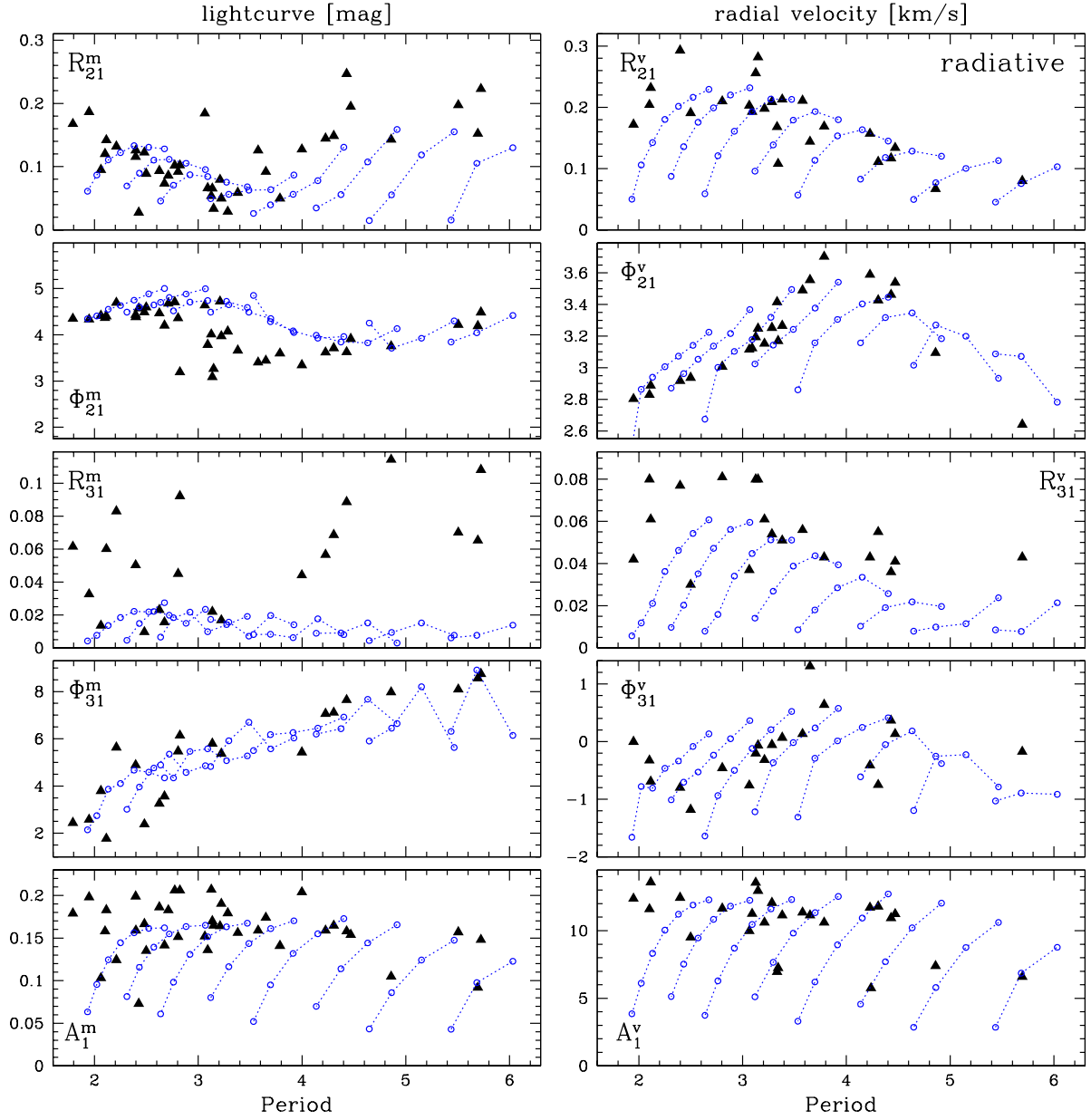


Fig. 3: Fourier coefficients of radiative models (open circles) compared to observations (filled triangles): *Left*: light-curve (mag) data; *Right*: radial velocity (km/s) data. The open circles connected by dotted lines refer to sequences with the same mass, starting from  $M = 4.25 M_{\odot}$  at the left to  $M = 6.25 M_{\odot}$  at the right in steps of  $0.25 M_{\odot}$ .

limb darkening factor ( $u_{\text{obs}} = u_{\text{cal}}/1.4$ ) to the calculated velocity values (Cox 1980).

### 3. RADIATIVE MODELS

As a first step we reexamine the difficulties encountered by radiative pulsation models, *i.e.*, models that for simplicity disregard all convection.

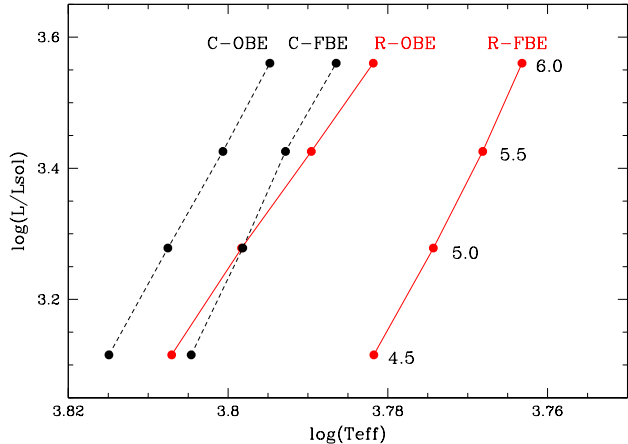


Fig. 4: Linear blue edges of *radiative* models (R-FBE and R-OBE) compared with those of convective models, series **A** (C-FBE and C-OBE). The labels on the right indicate the stellar masses.

As already discussed in the Introduction, a resonance between the first and the fourth overtone is responsible for the characteristic variations in the Fourier coefficients of both light- and radial velocity variations. The location of this resonance with respect to the pulsation period, which is of particular importance for the interpretation of non-linear results, can best be determined from linear results. In Fig. 2 the period ratio  $P_4/P_1$  is plotted as a function of  $P_1$  for each sequence of constant mass, and filled circles denote models with a stable overtone limit-cycle. Models close to the resonance center ( $P_1/P_4 = 2$ ), which fall within the region of stable overtone pulsation, appear between about  $P_1 = 4$  and  $5^d$ .

The results of the nonlinear radiative survey are summarized in Fig. 3 which depicts the low order Fourier coefficients, on the left for the light-curves, and on the right for the radial velocity curves. The observational data are represented by filled triangles, the theoretical models by open circles with dotted lines connecting the models of each sequence. We recall that the sequences consist of models with a given mass and luminosity, with  $T_{\text{eff}}$  decreasing and  $P_1$  increasing to the right.

Even though the overall picture is not at all disastrous, several severe problems are visible. First, and most strikingly, from the flatly distributed theoretical  $\Phi_{21}^v$  it is evident that the Z-shape of the observed data cannot be reproduced at all – a disagreement which has already been mentioned in the Introduction. In addition, the theoretical  $R_{21}^m$  values are too low for periods greater than 4 days, and the  $R_{31}^m$  are much too low overall. In contrast, the  $\Phi_{31}^m$  show reasonable agreement.

While the overall level of the pulsation amplitudes is set

by pseudo-viscosity, it is interesting that the behavior of the amplitudes  $A_1^m$  and  $A_1^v$  as a function of  $P_1$  follows the observations rather well.

For the radial velocity plots, the general agreement with observations is much better than for the light-curves. In particular, the calculated data fit the observed  $\Phi_{21}^v$  distribution. However, several models lie off the well defined observational distribution. The same discrepancy is also visible in all the other quantities. Below we show that the inclusion of convection gives better agreement.

In summary we thus corroborate the fact that radiative models are not able to reproduce satisfactorily the observational behavior of first overtone Cepheid pulsations.

### 4. CONVECTIVE MODELS

In the last few years it has become evident that the inclusion of convective energy transport is critical to the modelling of classical stellar pulsations, rather than just being necessary for stabilizing the models at low  $T_{\text{eff}}$ . The unpleasant consequence is that several free parameters ( $\alpha$ 's) have to be added to the former parameter-free radiative pulsation models. Theory unfortunately provides no guidance for choosing the values of these parameters, and therefore a calibration with observational data becomes necessary (*e.g.*, Stellingwerf 1984, Yecko *et al.* 1998, Feuchtinger 1999a).

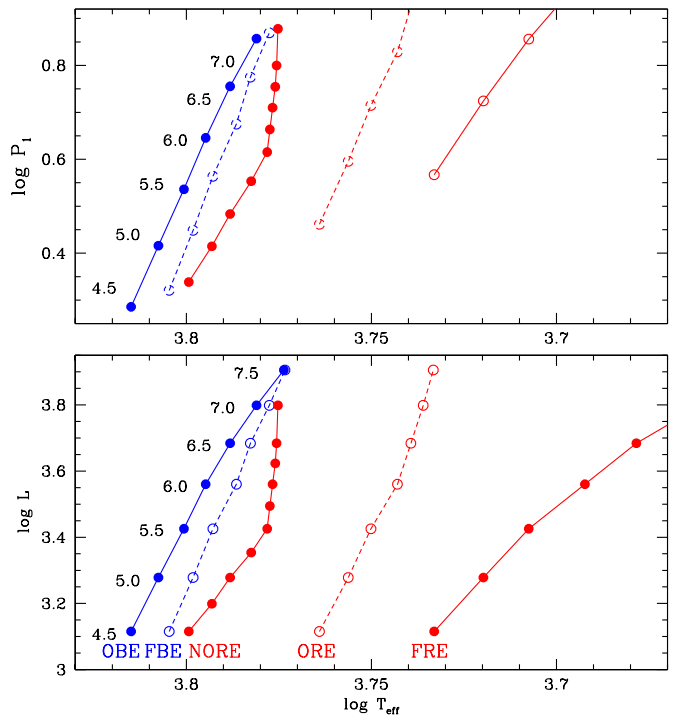


Fig. 5: Instability strip boundaries for *convective* models (series **A**), bottom: in the Log L - Log  $T_{\text{eff}}$  plane, top: in the Log  $P_1$  - Log  $T_{\text{eff}}$  plane. From left to right: (first) overtone linear blue edge (OBE), fundamental linear blue edge (FBE), nonlinear overtone red edge (NORE), overtone linear red edge (ORE) and fundamental linear red edge (FRE); the labels on left refer to the stellar masses.

For the present investigation we use the convection model according to Kuhfuß (1986) and Gehmeyr & Winkler (1992) in the version of Wuchterl & Feuchtinger (1999). Essentially the same model has been adopted by the Florida pulsation code (*cf.* Kolláth *et al.* 2000), but with a slightly different parameterization. A summary of the free parameters (subsequently termed  $\alpha$ 's) and the interrelations between the two sets of parameters are given in Table 1. For details we refer to the above cited references.

In the following we present five series of calculations, **A** through **E**, whose  $\alpha$ 's are given in Table 1. In order to reduce the multidimensional parameter space to a reasonable set of  $\alpha$ 's, we have pursued the following strategy. The parameters  $\alpha_s$ ,  $c_D$  and  $\alpha_c$  can be chosen to reduce the model to mixing length theory in the local static limit (Kuhfuß 1986, Wuchterl & Feuchtinger 1998), for the values  $\alpha_s = 1/2\sqrt{2/3}$ ,  $c_D = 8/3\sqrt{2/3}$  and  $\alpha_c = \alpha_s$ . The quantities  $\bar{\alpha}_s$ ,  $\bar{\alpha}_c$  and  $\bar{c}_D$  in Table 1 are given relative to these 'standard' values. We adopt the standard values in series **A**, and in addition set the mixing length parameter  $\alpha_{ML}$  to the widely used value of  $3/2$ . The parameter of the turbulent viscosity  $\alpha_\mu$  is used to adjust the pulsation amplitude. Turbulent pressure, overshooting, radiative losses and the convective flux limiter are disregarded in **A**. Series **B** investigates the effects of the flux limiter and series **C** the effects of radiative losses. Series **D** has much lower turbulent energy than series **A** and series **E** additionally includes the turbulent pressure and the turbulent flux. We wish to emphasize that the adopted choices of free parameters are by no means unique.

### Instability Strip

First we examine the influence of convection on the blue edge for series **A** and compare it to the radiative models. In Fig. 4 the radiative linear blue edges (R-FBE and R-OBE) are drawn as solid lines, and the convective ones (C-FBE and C-OBE) as dotted lines. In contrast to the frequently adopted notion that convection is only important near the red edge of the IS (*cf.* however Stellingwerf 1984), both the fundamental and the first overtone blue edges are shifted toward higher temperatures (toward the left in the figure) by about 350 K and 150 K for the fundamental and first overtone pulsations, respectively.

The complete *linear* topography of the IS for series **A** is presented in Fig. 5. The dotted lines refer to fundamental mode pulsation and the solid lines to the first overtone, filled/open circles to blue edge/red edges. These edges are somewhat sensitive to the values of the  $\alpha$ 's (*e.g.*, Yecko *et al.* 1998) and we show a comparison of the three series below.

The *nonlinear* first overtone red edge (NORE) is plotted as a dashed line in Fig. 5. It is located at considerably higher temperatures than the corresponding linear one. Slight smoothing has been applied because of the rather coarse steps in effective temperature. The low mass models (with  $M < 5.5M_\odot$ ) that are located at the right side of the NORE are double-mode pulsators, whereas the more massive ones ( $M > 5.5M_\odot$ ) pulsate in the fundamental mode. This modal change is the reason for the kink in the NORE (*cf.* Kolláth *et al.* 1998, Kolláth *et al.* 2000) for a detailed picture of the modal selection problem).

It is important to exercise considerable care that the computed overtone limit-cycles are indeed stable, and not just on a transient to either double-mode or to fundamental pulsations. These transients can be very long lasting and give an erroneous impression of steady behavior. A very efficient way of determining this stability with the 'analytical signal' method is discussed in Kolláth & Buchler (2000).

As expected and already discussed earlier (Yecko *et al.* 1998 and Kolláth *et al.* 1998), the fundamental and first overtone blue edges intersect at some point (at  $\sim 7.5 M_\odot$ ). This is consistent with the observational fact that the overtone Cepheid periods exhibit an upper limit, which is around  $P_1 = 6$  days for the Galaxy (with one single star found at  $7^{\text{d}}57$ ). The linear overtone period at the intersection point is  $8^{\text{d}}9$  here which is considerably higher than the observations suggest. However, the region above  $6.5M_\odot$  where stable overtone pulsations are possible is very narrow, which reduces the observational likelihood of such long period first overtone Cepheids. Furthermore the linear growth rates are found to be very small, and the corresponding nonlinear models exhibit tiny amplitudes (around  $0.03^m$  for the  $7 M_\odot$  sequence), since the pulsation amplitude scales with the square root of the growth-rate ( $A \sim \sqrt{\kappa}$ ). From the nonlinear survey we find that the maximum overtone period lies close to the observed one only when the pulsation amplitudes are in general agreement with observed ones. Our efforts to adjust the  $\alpha$ 's so as to lower the period at the intersection point, reduce the growth-rates and the pulsation amplitudes too much.

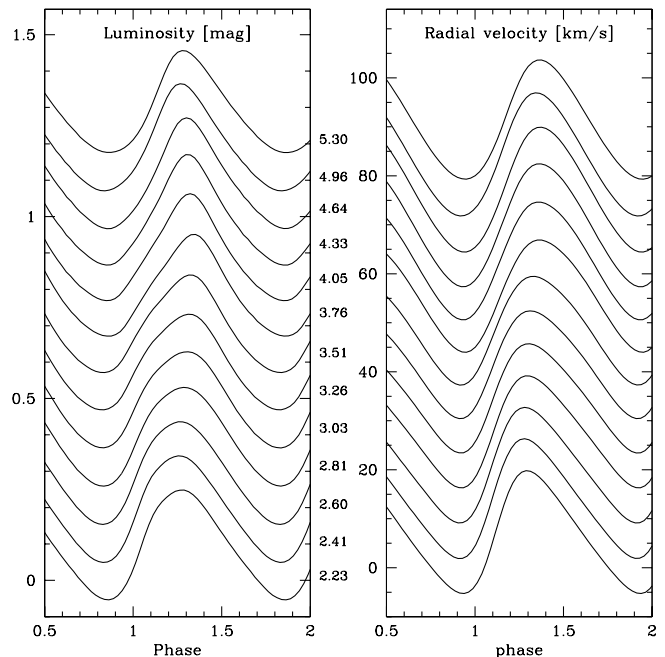


Fig. 7: *Left*: Light curves and *right*: radial velocity curves for a sequence parallel to the blue edge. The light-curves are shifted vertically by 0.1 mag and the radial velocity curves by 7 km/s. The curves are labelled with the periods.

Table 1: Free parameters of the time-dependent turbulent convection model. Columns 2 and 3 list the free parameters as defined in the Vienna and the Florida codes, respectively. Column 4 (interrelation) gives the Florida values as a function of the Vienna values. Columns **A** through **E** give the adopted parameter sets for our five model series in terms of the Vienna parameterization. No interrelation is given for the radiative cooling, as this effect is modelled slightly differently in the two codes. The parameters  $\bar{\alpha}_s$ ,  $\bar{\alpha}_c$  and  $\bar{c}_D$  are normalized to their standard values as given in the text.

| Physical meaning      | Vienna code      | Florida code     | interrelation                        | Series: | <b>A</b> | <b>B</b> | <b>C</b> | <b>D</b> | <b>E</b> |
|-----------------------|------------------|------------------|--------------------------------------|---------|----------|----------|----------|----------|----------|
| mixing length         | $\alpha_{ML}$    | $\alpha_\Lambda$ | $\frac{\alpha_{ML}}{\alpha_\Lambda}$ |         | 1.5      | 1.5      | 2.0      | 1.5      | 1.5      |
| turbulent source      | $\bar{\alpha}_s$ | $\bar{\alpha}_s$ | $\sqrt{\bar{\alpha}_s/\bar{c}_D}$    |         | 1        | 1        | 1        | 1        | 1        |
| turbulent dissipation | $\bar{c}_D$      | $\bar{\alpha}_d$ | $\bar{c}_D$                          |         | 1        | 1        | 1        | 4        | 4        |
| convective flux       | $\bar{\alpha}_c$ | $\bar{\alpha}_c$ | $\bar{\alpha}_c\bar{\alpha}_s$       |         | 1        | 1        | 1        | 1.5      | 1.5      |
| overshooting          | $\alpha_t$       | $\alpha_t$       | $\alpha_t/c_D$                       |         | 0        | 0        | 0        | 0        | 0.001    |
| turbulent viscosity   | $\alpha_\mu$     | $\alpha_\nu$     | $\alpha_\mu$                         |         | 0.25     | 0.33     | 0.35     | 0.50     | 0.50     |
| turbulent pressure    | $\alpha_p$       | $\alpha_p$       | $\alpha_p$                           |         | 0        | 0        | 0        | 0        | 2/3      |
| flux limiter          | $\alpha_L$       | $Y_{lim}$        | –                                    |         | 0        | 3        | 0        | 0        | 0        |
| radiative cooling     | $\gamma_R$       | $\alpha_R$       | –                                    |         | 0        | 0        | 3.5      | 0        | 0        |

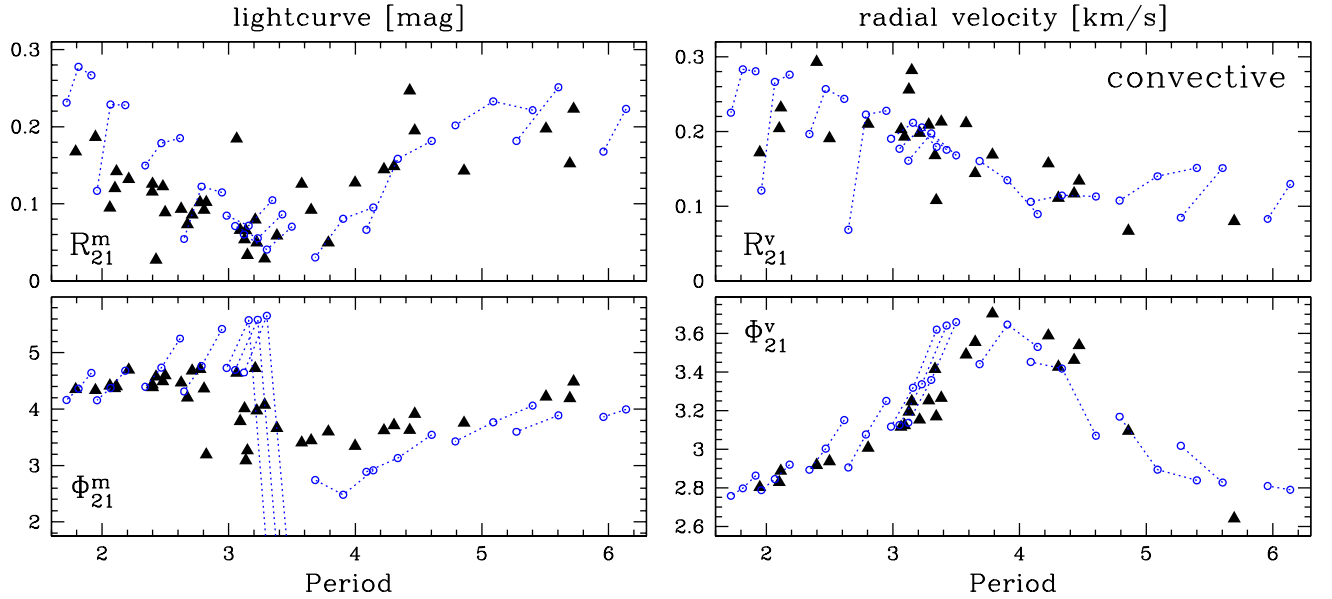


Fig. 6: Fourier coefficients of convective models, series **A** (open circles) compared to observations (filled triangles): *Left*: light-curve (mag) data; *Right*: Radial velocity (km/s) data. The open circles connected by dotted lines refer to sequences with the same mass (from left to right: 4.25, 4.50, 4.75, 5.00, 5.15, 5.20, 5.25, 5.50, 5.75, 6.0, 6.25, 6.50 $M_\odot$ ).

## Light-Curves and Radial Velocities

Fig. 6 displays the light- and radial velocity curve data for series **A**. Again we use filled triangles for the observations, while open circles represent our full amplitude pulsating models.

The light-curve Fourier coefficients for series **A**, exhibited on the left of Fig. 6, show great improvement with respect to the radiative series. The theoretical  $\Phi_{21}^m$  distribution attracts immediate attention with a very conspicuous jump around  $P_1 = 3^d4$ , in contrast to all the radiative models. In fact, the last points of the sequences 5 through 7 fall in the range 0.0–1.0, way below the scale. Even though the magnitude of the jump is considerably higher than what is observed, our model series reproduces qualitatively the observational  $\Phi_{21}^m$  behavior. In addition, all other light-curve Fourier coefficients show good overall agreement with observations. The values of the 31 Fourier coefficients are practically the same for series **A** through **E** and we refer to Fig. 10 for their display. Compared to the radiative models there is an average increase in  $R_{31}^m$  by almost a factor of 10, and for small periods, the convective models also display higher pulsation amplitudes and  $R_{21}^m$  values.

The radial velocity data on the right of Fig. 6 show good overall agreement as well. In particular, the  $R_{21}^v$  and  $\Phi_{21}^v$  distributions closely follow the observed ones, and they produce a much better match than the radiative models. For  $R_{31}^v$  and  $\Phi_{31}^v$  a similar behavior occurs, even though the  $R_{31}^v$  lie somewhat below the observed ones (*cf.* Fig. 10). However, the  $R_{31}^v$  are tiny which decreases the relevance of this deviation. The only perhaps significant discrepancy appears in the calculated amplitudes which, for the higher pulsation periods, are larger than the observed ones. This is also reflected in the larger  $R_{21}^v$ .

We have used the observed overall value of the pulsation amplitude to calibrate the  $\alpha$ 's (in practice  $\alpha_\mu$ ). When the amplitudes are increased beyond the observed values the jump in  $\Phi_{21}^m$  becomes increasingly weak and in disagreement with the observations.

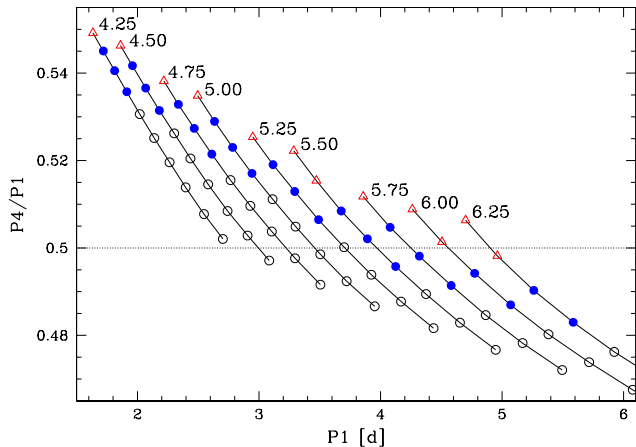


Fig. 8: Period ratio  $P_4/P_1$  versus pulsation period for convective models (series **A**). Open triangles denote vibrationally stable models. Filled/Open circles refer to models with a stable/unstable overtone limit-cycle. The labels on the right indicate the stellar masses.

The shapes of the calculated light- and radial velocity curves are displayed in Fig. 7 for a sequence of models running at 200 K distance parallel to the overtone blue edge.

Finally, we note that we have computed the same series **A** with the Florida convective (Lagrangian) pulsation code, and that the results are essentially identical. Despite the Lagrangian nature of the latter calculations the models show a very smooth behavior, in contrast to the radiative models for which the adaptive code is necessary (Buchler, Kolláth & Marom 1996) to give smooth light-curves (*cf.* also Sect. 5.1).

In summary we emphasize that the inclusion of convection is crucial for a successful quantitative modelling of the pulsational properties of first overtone Cepheids, in particular of the Fourier decomposition coefficients of the light- and radial velocity curves.

## Location of Resonance

We return here to the important question of whether the resonance center is near  $P_1 = 3^d2$  as suggested by the light-curves (Antonello & Poretti 1986) or near  $4^d6$  as the radial velocity data indicate (Kienzle *et al.* 1999).

First, we note that our calculations which used the Schaller *et al.* M–L relation ( $\log(L/L_\odot) = 0.79 + 3.56 \log(M/M_\odot)$ ), reproduce the observed shift with period between the light-curve and the radial velocity curve  $R_{21}$  and  $\Phi_{21}$ . From our calculated linear period ratios we should therefore be able to locate the resonance center, and resolve this issue. (We stress that it is important to use the same code, *i.e.*, the same differencing scheme and the same mesh to compare the hydrodynamics results to the linear periods). We note in passing that the relative differences between the nonlinear and the linear periods are at most +0.4%.

The linear period ratios  $P_4/P_1$  versus pulsation period for our convective series **A** are shown in Fig. 8. The filled circles denote models with a stable nonlinear overtone limit-cycle. Note that our nonlinear first overtone IS is very narrow. We shall return later (§6) to the importance of the narrowness. Only two of our mass sequences (5.5 and 5.75  $M_\odot$ ) can undergo stable overtone pulsations with periods near the resonance center (in contrast to the radiative models of Fig. 2). The corresponding pulsation periods reveal the resonance to be located around  $P_1 = 4^d2 \pm 0.3$ , in fact very close to the value of  $4^d6$  that Kienzle *et al.* (1999) had conjectured.

Our calculations leave no doubt that the  $P_1/P_4 = 2$  resonance is responsible for the observed structure of the light and radial velocity Fourier coefficients, and that the resonance is located in the vicinity of  $P_1 = 4^d2$ .

It is somewhat surprising that the 2:1 resonance with the fourth overtone has such a pronounced effect on the Fourier data, because after all this overtone is so strongly damped. It has a relative damping rate per pulsation period of  $\kappa_4 P_0 \sim -0.4$  in the vicinity of the resonance, *i.e.*, its amplitude would decay by 33% in one pulsation period.

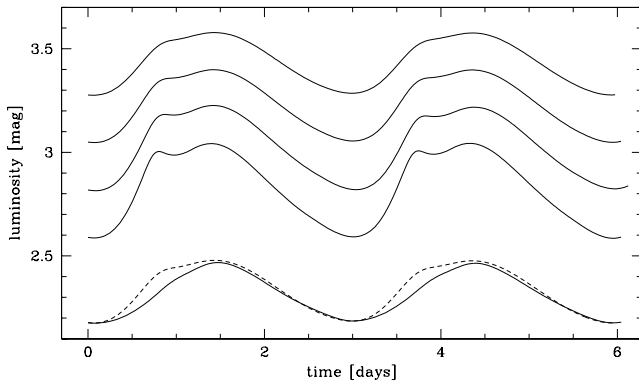


Fig. 9: Effect of pulsation amplitude on the light-curve for a series **A** model located at the  $\Phi_{21}^m$  jump. Upper four solid lines, have decreasing turbulent viscosity, 0.25 (top) to 0.1 (bottom) in steps of 0.05. The lowest solid line shows the corresponding light-curve with the convective flux limiter included, the dashed line refers to the same model without the flux limiter.

## 5. SENSITIVITY TO NUMERICAL AND PHYSICAL INPUT

### 5.1. Lagrangean versus adaptive mesh

We mentioned in the preceding paragraphs that a comparison between convective Lagrangean and adaptive calculations reveals no differences, as far as first overtone Cepheid models are concerned. This comes as no surprise, because pulsation amplitudes are rather small, and no strong shock waves appear in the dynamics which would require a more elaborate numerical treatment. Moreover, the inclusion of convective energy transport considerably smoothes the sharp features in the combined H–He ionization zone which are a well known headache for radiative modelling.

However, a word of caution is necessary here. As already discussed in detail in Feuchtinger & Dorfi (1994) and Buchler, Kolláth & Marom (1996), adaptive models suffer from advection errors due to the non-Lagrangean motion of the cell boundaries. These errors are particularly severe in the interior where the cell-masses increase rapidly. In order to keep these errors small, the interior part of the model has to be treated as Lagrangean. The switching point between Lagrangean and adaptive zoning therefore has to be chosen with some care, as advection errors can considerably influence the dynamical behavior and ultimately the morphology of the light- and radial velocity curve. By comparing the adaptive results to Lagrangean results we checked in detail that our results are not vitiated by advection errors.

### 5.2. Radiation hydrodynamics versus equilibrium diffusion

A standard radiation diffusion equation for radiative transport is much more convenient and faster than a time-dependent treatment of radiative transfer (radiation hydrodynamics). Since both codes are available, it has seemed interesting to check whether the simplified diffusion was adequate for pulsational behavior. On the basis

of the study of several sequences of models we find that, apart from small changes in the pulsation amplitudes, the results are essentially the same for both treatments. In particular no noticeable effect on the low order Fourier coefficients has been found. A radiation diffusion treatment is therefore fully adequate.

### 5.3. The M–L Relation

Our results do not depend sensitively on the chosen M–L relation as long as the latter puts the resonance in the right place. This is so because the agreement of the hydrodynamical results with the observations necessarily puts the resonance at the right place and thus fixes the zero-point of the M–L relation (Buchler *et al.* 1996). The properties of the models depend very little on the slope of the M–L relation because of the relatively narrow mass range of the overtone Cepheids.

### 5.4. Convection and the $\alpha$ parameters

In the following we discuss how several of the convective parameters influence the behavior of first overtone Cepheid models and in particular the Fourier coefficients of the light- and radial velocity curves.

#### Series **B**

A striking feature of the convective models of series **A** in Section 4 is the large jump of the  $\Phi_{21}^m$ , and it is interesting to see whether the size of this jump can be decreased to observed values by changing the  $\alpha$ 's.

First of all it is instructive to investigate whether there are any peculiar features in the light-curve structure that are connected with that jump. Fig. 9 (solid line at the top) shows the light-curve of a model of series **A** which is located just to the left of that jump. The light-curve exhibits a shoulder on the rising branch that is absent in the observed light-curves. This shoulder appears only in models near the  $\Phi_{21}^m$  jump and no corresponding feature can be found in the radial velocity curve. If the pulsation amplitude of the model is increased beyond the observed value through a decrease in the turbulent viscosity, the shoulder becomes increasingly pronounced, as the lower solid lines indicate. Eventually a spike develops that is similar to the one found in the convective models of RR Lyrae stars (Feuchtinger 1999b).

In order to cure the problem of the spike Wuchterl & Feuchtinger (1998) capped the size of the correlations  $\langle s'u' \rangle \approx \langle h'u' \rangle$  to which both the source of turbulent energy and the convective flux are proportional (flux limiter). In series **B** we apply the same type of limiter to the first overtone Cepheid models. However, in contrast to the RR Lyrae models we use a higher value of  $\alpha_L = 3$  instead of 1 which diminishes the effect of the flux limiter and hence only slightly changes the convective structure of the models. Because the limiter reduces the amount of convection and therefore also the dissipation, we need to increase the turbulent viscosity parameter  $\alpha_\mu$  from 0.25 to 0.33 to maintain the same pulsation amplitudes.

The resulting change in the light-curve structure can be inferred from the bottom of Fig. 9 which plots the flux limited light-curve (solid line) as compared to the non-limited case (dashed line). The Fourier analysis yields a drop of  $\Phi_{21}^m$  from 5.42 to 4.20 for the limited model. The



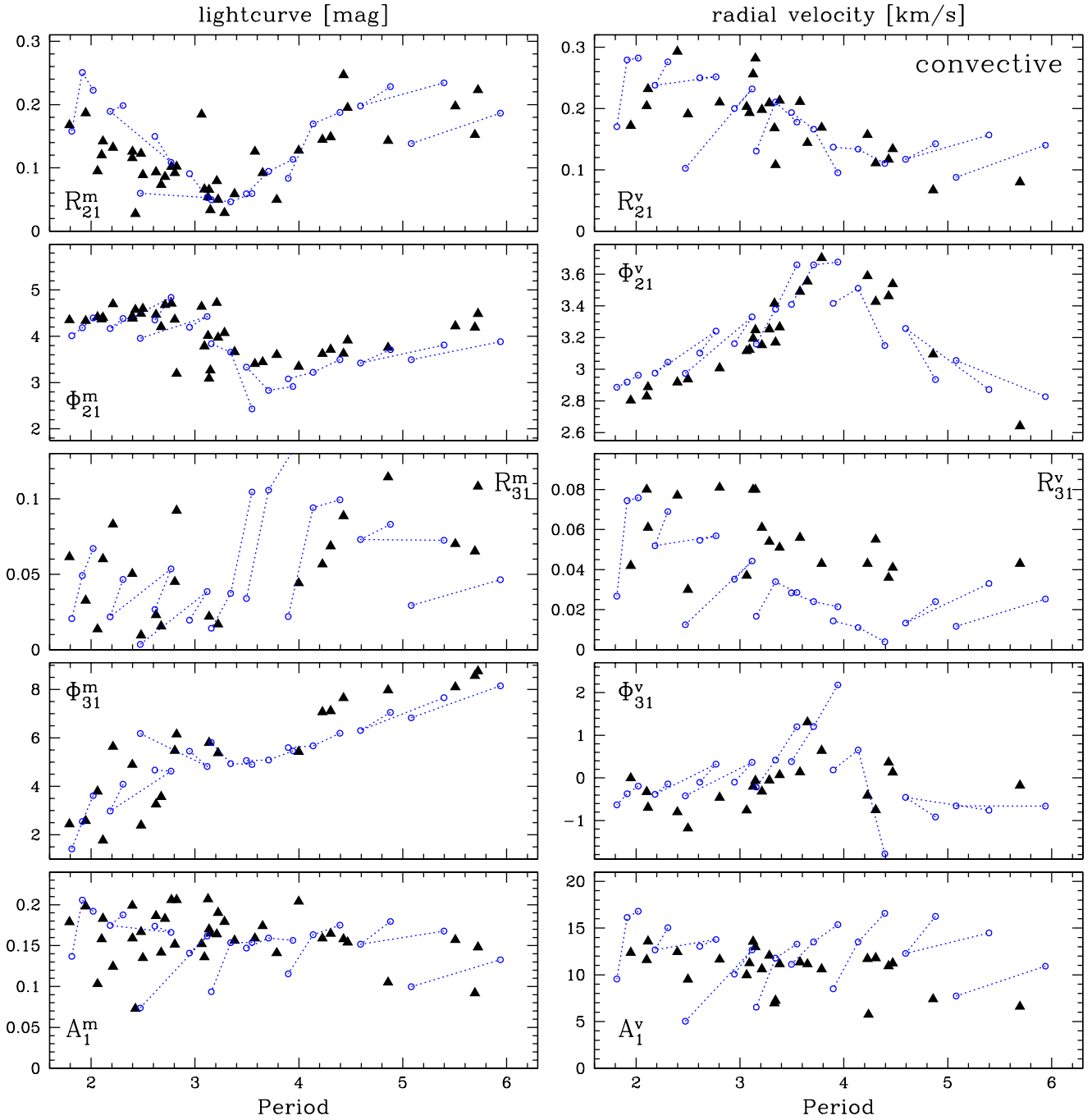


Fig. 10: Fourier coefficients  $R_{21}$  and  $\Phi_{21}$  of convective models series **B** with the convective enthalpy flux limiter (open circles) compared to observations (filled triangles): *Left*: light-curve (mag) data; *Right*: Radial velocity (km/s) data. The open circles connected by dotted lines refer to sequences with the same mass (from left to right: 4.25, 4.50, 4.75, 5.00, 5.15, 5.25, 5.50, 5.75, 6.00, 6.25  $M_{\odot}$ ). For comparison purposes the scales are the same as in Figs. 7 and 12.

comparison of the whole flux-limited sequence with observations is given in Fig. 10. The bottom panels show  $R_{31}$ ,  $\Phi_{31}$  and  $A_1$ . It turns out that the inclusion of the flux limiter decreases the jump in  $\Phi_{21}^m$  considerably, while all other quantities remain almost unaffected. Clearly the best results are obtained when a flux limiter is included.

All our attempts to achieve the same effect as obtained with a flux limiter by using various combinations of  $\alpha$ 's have proved in vain. Essentially the same was found for RR Lyrae stars (Feuchtinger 1999b). This state of affairs is somewhat disconcerting because of the *ad hoc* nature of the flux limiter, and its cause may well be found in the oversimplified nature of our 1D treatment of turbulent convection.

### Series C

Another effect that was omitted in the model series **A** of Section 4 concerns the decrease of turbulent kinetic energy through radiative losses. This effect is important when the radiative diffusion time scale becomes comparable to or smaller than the typical eddy rise time, *i.e.*, when the Péclet number is small (This effect is treated differently in the Vienna code (Wuchterl & Feuchtinger 1998) and in the Florida code (Buchler & Kolláth 2000; Kolláth *et al.* 2000) who follow the recipe of Canuto & Dubikov 1998). A nonzero value of the corresponding parameter  $\gamma_r$  causes both a decrease of the convective flux and the turbulent kinetic energy. In our sequence **C** we use  $\gamma_r = 3.5$ . To compensate for the resulting decrease of dissipation and to avoid too large an instability strip and too large pulsation amplitudes, we increase the mixing length parameter  $\alpha_{ML}$  from 1.5 to 2 and the turbulent viscosity  $\alpha_\mu$  from 0.25 to 0.35 (series **C**, see also Table 1). This yields approximately the same pulsation amplitudes as obtained without the Péclet correction.

The influence on the linear IS boundaries is shown in Fig. 12. The solid lines refer to models including radiative losses (**C**), dashed to the original sequence (**A**), and **F** and **O** denote the fundamental and first overtone mode, respectively. Both fundamental and overtone blue edges are shifted to the blue by the same amount of about 100K. In contrast, the average fundamental red edge shift of about 550 K to the blue edge is much larger than the corresponding 200 K for the overtone red edge. Considering the average linear IS widths (taken at  $6 M_\odot$ ) we end up with 580 K for the first overtone and 780 K for the fundamental, compared to 700 K and 1200 K, respectively, for the series without radiative losses. Consequently, the inclusion of radiative losses has a differential effect on fundamental and first overtone growth rates, which is important for the calibration of the whole Cepheid picture (*cf.* Section 7).

The nonlinear results for series **C** are shown in Fig. 11 and compared to observed values. Even though the topology of the IS is changed considerably, the influence on the Fourier coefficients is not conspicuous. In particular the large jump of  $\Phi_{21}^m$  is only slightly reduced compared to series **A** in Fig. 6. Additionally, the position of that jump and also the maximum of  $\Phi_{21}^m$  remain at the same place. Bearing in mind that several constraints involving fundamental and double-mode pulsations have not been considered so far, such insensitivity is welcome because it provides leeway for matching additional constraints (*cf.*

Section 7).

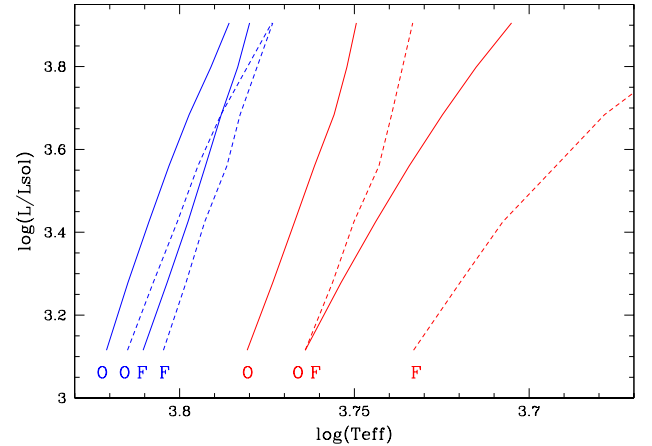


Fig. 12: Linear IS boundaries for convective model series **C** (which include radiative losses, solid lines) compared to series **A** (dashed lines) in the HR diagram.

### Series D and E

The Kuhfuß standard choice for  $\alpha_s$ ,  $\alpha_c$  and  $c_D$  which gives the mixing length theory (MLT) limit in the local and static case, leads to rather high values of the turbulent kinetic energy  $e_t$ . For a typical hydrostatic initial model  $e_t$  peaks around  $0.55e$  in the H ionization zone and at  $0.25e$  in the HeI zone, where  $e$  denotes the internal energy. Dynamical effects might lead to even higher values of  $e_t$  during some stages of the pulsation cycle (*cf.* Buchler, Yecko, Kolláth & Goupil 1999, Figs. 1 and 2). The corresponding convective Mach numbers  $\sqrt{2/3} e_t/c_s$ , where  $c_s$  denotes the adiabatic sound-speed, reach values of about 0.7. Clearly one is close to the limit of validity of our convection model, which, by disregarding pressure fluctuations, assumes a convective element always to be in pressure equilibrium with its surroundings. It is therefore interesting to compute a model series with considerably lower  $e_t$ . This can be accomplished in different ways because several  $\alpha$  parameters (*viz.*  $\alpha_{ML}$ ,  $\alpha_s$  and  $c_D$ ) exhibit a strong influence on  $e_t$ .

In series **D** of Table 1 we increase the dissipation parameter  $c_D$  by a factor of 4, which leads to an average reduction of  $e_t$  by a factor of 3. At the same time we increase  $\alpha_c$  to 1.5 times its original value (series **A**), which results in approximately the same convective flux structure. Moreover, in order to obtain the right pulsation amplitudes one needs to increase the turbulent viscosity. Despite these rather dramatic changes of the  $\alpha$ 's only minor changes in the pulsational properties of the models are found.

Series **E** includes both turbulent kinetic energy flux  $F_t$  and turbulent pressure  $p_t$ , but has the same  $\alpha$ 's as the low  $e_t$  series **D**. The flux  $F_t$  has only a small effect on the pulsation for reasonable values of  $\alpha_t$ , *i.e.*, as long as the convection zones do not invade the outer boundary. The turbulent pressure is also unimportant as long as it remains small compared to the gas pressure. The inclusion of these quantities thus causes neither significant changes

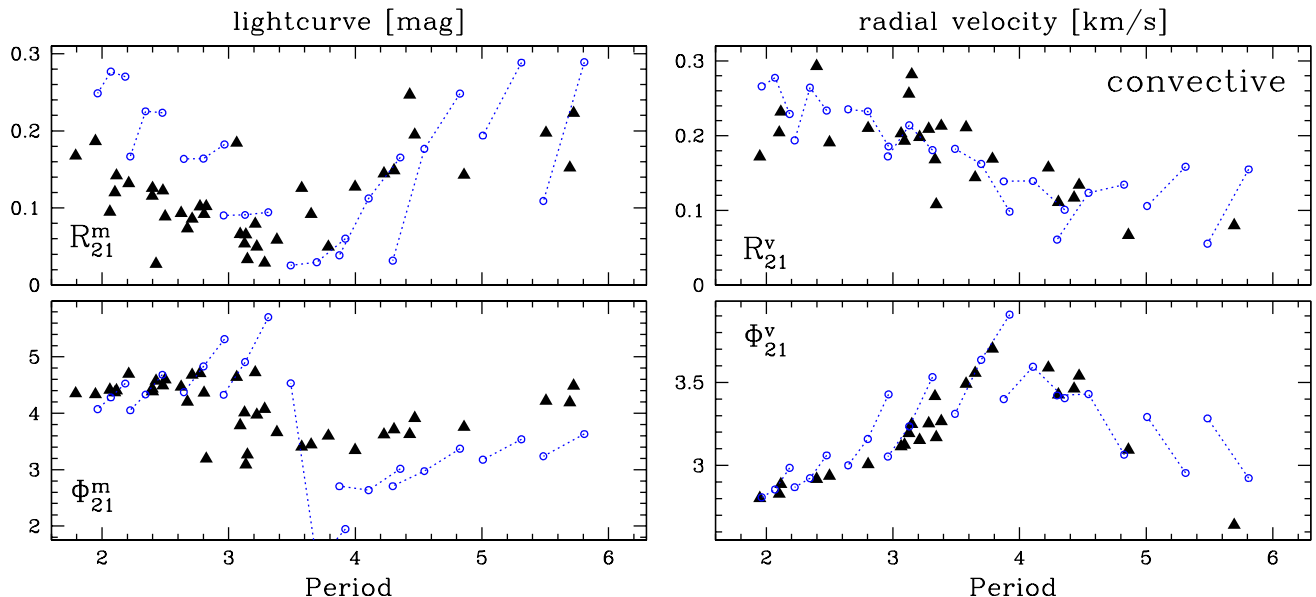


Fig. 11: Fourier coefficients  $R_{21}$  and  $\Phi_{21}$  of convective models (series **C**) that include radiative losses (open circles) compared to observations (filled triangles): *Left*: light-curve (mag) data; *Right*: Radial velocity (km/s) data. The open circles connected by lines refer to sequences with the same mass (from left to right: 4.50, 4.75, 5.00, 5.25, 5.50, 5.75, 6.00, 6.25, 6.50, 7.00  $M_{\odot}$ ). For comparison purposes the scales are the same as in Figs. 8 and 10.

in the topography of the instability strip nor in the Fourier coefficients.

For some choice of the parameters  $\alpha_{ML}$ ,  $\alpha_s$ ,  $\alpha_c$  and  $c_D$  the turbulent kinetic energy  $e_t$  is very large. Then, because  $p_t = \alpha_p \rho e_t$ , the turbulent pressure can get as large or even larger than the gas pressure for the standard value of the parameter  $\alpha_p = 2/3$ . Since a much smaller value of  $\alpha_p$  does not seem appropriate in this picture (/eg Baker 1987) this suggests that it would be preferably to use sets of  $\alpha$ 's that yield a lower  $e_t$  profile and a reasonable  $p/p_t$  ratio. On the other hand, such a problem might also reflect the limitations of the simple 1D model of convection that we use.

## 6. WIDTH OF THE INSTABILITY STRIP

We recall that the left (hot) side of the IS determined by the linear growth-rates (which change sign there), but that the red (cool) edge is determined by nonlinear effects, namely instability of the limit-cycles. At low masses (and luminosities) the overtone limit-cycles become unstable to double-mode pulsations, and at higher masses they turn into fundamental pulsations (Udalski *et al.* 1987, Kolláth *et al.* 2000).

The comparison of our calculated Fourier data with the observations suggests that the overtone IS must be very narrow. Indeed, Figs. 6, 10 and 11 show a strong tendency for the computed values of the  $\Phi_{21}^m$  (dotted lines) to climb above the observed values as the period of the models increases along each mass sequence, in particular the low mass sequences. Had we chosen  $\alpha$ 's that yield a much broader IS then the disagreement of the computed values with the observations would have been severe.

It is somewhat puzzling that the observations show practically no low amplitude overtone Cepheids (Fig. 3), neither in light nor in radial velocity, and neither at the blue edge nor at the red edge. Of course there is some obser-

vational bias against low amplitude pulsators but we do not believe that it can account for the observed deficiency. In Buchler, Kolláth & Feuchtinger (2000) we show that the build-up of the pulsation amplitude can be delayed by stellar evolutionary effects. But this happens only on the redward entry into the IS. Another possibility is that the behavior of the growth-rates with  $T_{\text{eff}}$  is much steeper than our calculations indicate. If this were the reason it would point to an inadequacy of the simple 1D treatment of convection that we use.

## 7. FUNDAMENTAL MODE PULSATORS

Even though our first overtone Cepheid models display good agreement with observations, this tells only one part of the story. A comprehensive model for Galactic Cepheids will have to reproduce the observed behavior of the complete modal behavior (fundamental, overtone and double-mode pulsations) throughout the whole IS. Accordingly, further constraints such as the Hertzsprung progression of the Fourier coefficients of the fundamental Cepheid light- and radial velocity curves (connected with the  $P_0/P_2 = 2$  resonance), or the location and properties of the double-mode pulsations need to be included. Such a calibration is beyond the scope of this paper. There is no *a priori* guarantee that our adopted parameter sets, which give good results for first overtone Cepheids, also work for fundamental Cepheids. We thought it useful to ascertain that with our  $\alpha$ 's the fundamental mode models are at least reasonably good. On the basis of a few sequences of models we find that even though the agreement is not perfect, the main features in the Fourier coefficients can be reproduced. There is therefore hope that future work will be able to determine a set of  $\alpha$ 's that will yield a comprehensive picture of the Galactic Cepheids.

## 8. LOW METALLICITY CEPHEIDS

The Magellanic Clouds are thought to be metal-deficient compared to the Galaxy, and presumably so are the SMC and LMC Cepheids. Nevertheless, the observed characteristics of these Cepheids (*e.g.*, stellar parameters, pulsation amplitudes, position of resonances, double-mode behavior, etc.) are very close to those of their Galactic siblings. However, current models show a strong metallicity ( $Z$ ) dependence that is in conflict with the observed behavior (*e.g.*, Buchler, Kolláth, Beaulieu & Goupil 1996, Buchler 2000). This issue will be addressed in detail in a forthcoming paper.

## 9. SUMMARY AND CONCLUSIONS

In this paper we have addressed the modelling of Galactic first overtone Cepheids with two different state-of-the-art stellar pulsation codes. Both codes include a treatment of time-dependent convective energy transfer, *viz.* the Vienna and the Florida codes. A reexamination of radiative models with an adaptive mesh and radiation hydrodynamics code reveals no improvement when compared with the

simpler Lagrangean radiative diffusion code. In particular, the conspicuous Z-shape of the  $\Phi_{21}^m$  with period cannot be reproduced with radiative modelling.

In contrast, we demonstrate that with the inclusion of convective energy transport it is possible to reproduce the observed behavior of Galactic first overtone Cepheids. The Schaller *et al.* M–L relation that we have used here puts both the overtone  $P_1/P_4=2$  and the fundamental  $P_0/P_2=2$  resonances in approximately the right places as the agreement between the calculated and the observed Fourier data show. With a slight adjustment of the M–L relation the agreement with the observations could be further improved. In particular our models reveal that the  $P_1/P_4 = 2$  resonance which is responsible for the structure in the Fourier coefficients, is located at pulsation periods in the vicinity of  $P_1 = 4^{\text{d}}2$ , as conjectured by Kienzle *et al.* (1999) on the basis of their radial velocity data.

## 10. ACKNOWLEDGEMENTS

This work has been supported by NSF (grant AST 9819608) and by OTKA (T-026031).

## REFERENCES

- Aikawa T., Antonello E., Simon N.R., 1987, AA 181, 25  
 Alexander, D. R. & Ferguson, J. W. 1994, ApJ 437, 879  
 Antonello, E. & Aikawa, T. 1993 AA 279, 119  
 Antonello, E. & Aikawa, T. 1995 AA 302, 105  
 Antonello, E. & Poretti, E. 1986, AA, 169, 149  
 Baker, N.H. 1987, in *Physical Processes in Comets, Stars and Active Galaxies*, Eds. W. Hillebrandt, E. Meyer-Hofmeister & H.-C. Thomas, p. 105 (Berlin: Springer-Verlag).  
 Beaulieu, J.P. *et al.* 1995, AA 303, 137  
 Buchler, J. R., 1993, in *Nonlinear Phenomena in Stellar Variability*, Eds. M. Takeuti & J.R. Buchler (Kluwer: Dordrecht), repr. from ApSS 210, 1  
 Buchler, J. R., 2000, in "The Impact of Large-Scale Surveys on Pulsating Star Research", Proc. IAU Colloquium 176, Budapest 1999, ASP Conf. Ser., Eds. L. Szabados & D.W. Kurtz, 203, p. 343  
 Buchler, J. R. & Goupil, M. J. 1984, ApJ 279, 394  
 Buchler, J.R., Kolláth, Z., Beaulieu, J.P. & Goupil, M.J. 1996, ApJL 462, L83  
 Buchler, J. R. & Kolláth, Z., 2000, in *Astrophysical Turbulence and Convection*, Eds. J.R. Buchler & H. Kandrúp, Annals of the New York Academy of Sciences, Vol. 898, p. 39  
 Buchler, J.R., Kolláth, Z. & Feuchtinger, M. U. 2000, AA, submitted  
 Buchler, J.R., Kolláth, Z. & Marom, A. 1996, Astrophys. Space Sci. 253, 139  
 Buchler, J.R. & Kovács, G. 1986, ApJ 303, 749  
 Buchler, J. R., Moskalik, P. & Kovács, G. 1990, ApJ 351, 617  
 Buchler, J. R., Yecko, P., Kolláth, Z. & Goupil, M. J. 1999, in *Theory and Tests of Convection in Stellar Structure*, ASP Conf. Ser. 173, Eds. A. Gimenez, E.F. Guinan & B. Montesinos, p. 141  
 Canuto, V. M. & Dubikov, M., 1998, ApJ 493, 834  
 Cox, J. P. 1980, *Theory of Stellar Pulsation*, (Princeton: Univ. Press)  
 Dorfi, E. A. & Feuchtinger, M. U. 1999, AA 348, 815  
 Feuchtinger, M.U., 1998, AA 337, L29  
 Feuchtinger, M.U., 1999a, AAS 136, 217  
 Feuchtinger, M.U., 1999b, AA 351, 103  
 Feuchtinger, M.U. & Dorfi, E.A., 1994, AA 291, 225  
 Feuchtinger, M.U. & Dorfi, E.A., 2000, in "The Impact of Large-Scale Surveys on Pulsating Star Research", Proc. IAU Colloquium 176, Budapest 1999, Eds. Laszlo Szabados and Don Kurtz, ASP Conf. Ser., 203, p. 334  
 Gehmeyr, M. & Winkler, K.-H. A. 1992, AA 253, 92  
 Hertzprung E. 1926, Bull. Astr. Inst. Netherlands 3, 115  
 Iglesias, C.A. & Rogers, F.J., 1996, ApJ, 464, 943.  
 Kienzle, F., Moskalik, P., Bersier, D. & Pont, F. 1999, AA 341, 818  
 Kolláth, Z., Beaulieu, J. P., Buchler, J. R. & Yecko, P., 1998, ApJ 502, L55  
 Kolláth, Z. & Buchler, J. R., 2000, in *Nonlinear Studies of Stellar Pulsation*, Eds. M. Takeuti & D.D. Sasselov, Astrophysics and Space Science Library Series, Kluwer (in press)  
 Kolláth, Z., Buchler, J.R., Szabó, R. & Csúbrý, Z., 2000, ApJ, (submitted)  
 Kovács, G. & Buchler, J.R., 1989, ApJ, 346, 898  
 Krzyt, T., Moskalik, P., Gorynya, N. & Samus, N. 2000, (in preparation)  
 Kuhfuß, R., 1986, AA 160, 116  
 Moskalik, P., Buchler, J.R. & Marom, M. 1992, ApJ 385, 685  
 Poretti, E., 1994, AA, 285, 524  
 Schaller G. & Buchler, J. R. 1994, unpublished preprint, A *Hydrodynamical Survey of s-Cepheid Pulsations*  
 Schaller, G. Schaeerer, D. Meynet, G. & Maeder, A. 1992, AAS 96, 269  
 Simon, N. R. & Schmidt, E. G., 1976, ApJ 205, 162  
 Stellingwerf, R. F. 1984, ApJ 277, 322  
 Udalski, A., *et al.* 1997, Acta Astr 47, 1  
 Welch, D.L., Alcock, C., Bennett, D.P., *et al.* , 1995, in IAU Coll. 155 "Astrophysical Applications of Stellar Pulsation", Eds. R.S. Stobie & P.A. Whitelock, ASP Conference Series, Vol. 83, p. 232  
 Wuchterl, G. & Feuchtinger, M. U. 1998, AA 340, 419  
 Yecko, P.A., Kolláth, Z. & Buchler, J.R., 1998, AA 336, 553